rail vehicle dynamic modelling; creep forces calculation; Nadal's criterion

Stasys STEIŠŪNAS*, Gintautas BUREIKA
Vilnius Gediminas Technical University
Saulėtekio al. 11, LT–10223 Vilnius, Lithuania
**Corresponding author*. E-mail: stasys.steisunas@vgtu.ltt

STUDY OF FREIGHT WAGON RUNNING DYNAMIC STABILITY TAKING INTO ACCOUNT THE TRACK STIFFNESS VARIATION

Summary. Authors analysed the rail dynamic models of rail vehicle and surveyed the features of the system "vehicle-track" modelling. Algorithms of creep forces calculation were examined. Four-axle freight wagon movement on the straight track and on curves corresponding to the given vertical and transversal track irregularities was modelled by software tool "Universal Mechanism". Authors examined the track stiffness influence on the vehicle moving stability/safety parameters at different speed, vehicle weight and track irregularities considering different wear rail profiles. Finally, basic conclusions and recommendations are given.

ИССЛЕДОВАНИЕ ДИНАМИЧЕСКОЙ СТАБИЛЬНОСТИ ДВИЖЕНИЯ ГРУЗОВОГО ВАГОНА ПРИ ИЗМЕНЕНИЯХ ЖЕСТКОСТИ ЖЕЛЕЗНОДОРОЖНОГО ПУТИ

Аннотация. Авторы проанализировали динамические модели рельсовых экипажей и рассмотрели особенности моделирования системы «вагон-путь». Рассмотрены алгоритмы расчета сил крипа. С помощью программного пакета «Универсальный механизм» было смоделировано движение четырехосного грузового вагона по прямой трассе и по кривой с учетом вертикальных и горизонтальных неровностей рельсовых нитей. Авторы исследовали влияние жесткости железнодорожного пути на параметры стабильность/безопасность движения рельсового экипажа, движущегося с разной скоростью, с разной массой вагона и с учетом профилей рельсов различного износа. В конце сформулированы основные выводы и рекомендации.

1. INTRODUCTION

In the past the dynamical analysis of the system "vehicle–track" was usually split up into two parts: short and long term dynamics. On the one hand , the vehicle dynamics including vehicle disturbances were investigated, but using very simple track models [11]. On the other, the track dynamics including track disturbances were analysed, but assuming very simple vehicle models. However, today and in the near future an integrated analysis of the entire system is required, where all components of the system have the same level of accuracy and where different time scales of the subsystems are considered by special computational methods. Analysis based on different types of models for vehicles and various tracks. Then, the wheel-set dynamics and the track dynamics are considered in more detail. Finally, integrated models of entire system will be collated (Fig. 1).

The interaction of these components can be analysed using an adequate mathematical description based upon reliable physical models. After the critical speed problem has been solved, current research in the field of railway systems deals with the influence of the train-track dynamics on the development of disturbances. Here, two different time scales occur. One can distinguish between short time vehicle-track dynamics and long-term dynamics of degradation and damage processes, both interacting with each other.

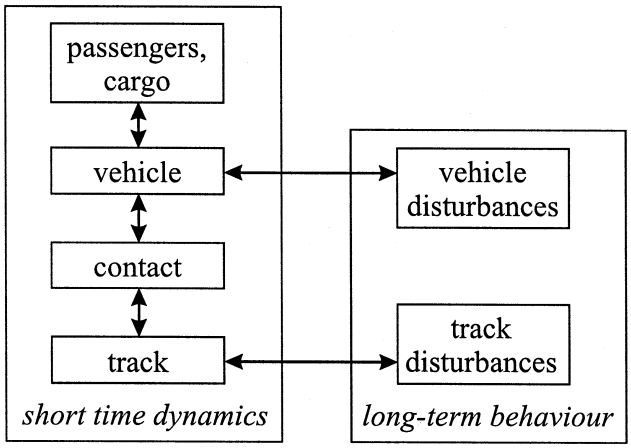

Fig. 1. Block diagram of the vehicle-track system showing the subsystems [11]
Рис. 1. Блок-схема системы рельсовый экипаж-путь [11]

Though these phenomena are well known for a long time, they appear much more pronounced in modern high speed transportation systems.

The vehicle-track system is generally composed of two parts, namely the upper structure and the lower structure. In a typical analysis, these two parts are connected as a coupled system that accounts for interaction between the wheel and rail [1]. The adoption of a realistic track model has a large influence on the computational cost of the simulation [2, 7]. A design providing good ride quality even on non-perfect track is preferred to avoid excessive track maintenance costs when speeds are higher [9].

The rigid multibody models are appropriate in the low frequency range of about 0–50 Hz. Today exists three powerful software tools with particular advantages for the modelling of rail vehicle systems: SIMPAC, ADAMS/VI-RAIL and UNIVERSAL MECHANISM (UM).

Significant are accurate models with only a few degrees of freedom like the finite element model of a wheel-set developed by Fingberg [3]. An elastic bogie frame with rigid wheel-sets has been recently investigated for a stress and fatigue analysis.

The classical continuous models of infinite length have been extensively investigated. They date back to Timoshenko in 1915. He studied an infinite Bernoulli-Euler beam on an elastic Winkler foundation under static and dynamic loads. Later found that in the speed-frequency plane of force parameters there exist 22 regions of different wave solutions [11]. The continuous models have been improved from one layer models up to three layers and continuous half-space models [6]. In recent publications the half-space has been replaced by springs with stiffness depending on frequency and wavelength [8].

The discrete models take into account the discrete rail support by the sleepers. They can be divided into models of infinite and finite length. One possibility to extend the infinite continuous models and approximate the discrete sleeper support is provided by a Fourier series expansion [11]. An alternative is the modelling by periodic structures, whose mathematical treatment is known from other fields of engineering. Models of this type have been developed by Popp and authors [12].

2. ESTIMATION METHODS OF WHEEL–RAIL CONTACT FORCES

2.1. Method for computation of rail deflections and contact forces

A rail is considered in UM as a massless force element. This means, both stiffness and damping of the rail is taken into account, but not the inertia properties. Generalized coordinates are not introduced for the rail and its lateral and vertical deflections must be computed from the equilibrium equations. The following assumptions take place [16]:

1) deflections of a rail for different wheel-sets are independent and can be computed separately;
2) deflections of the left and right rails are independent;
3) rail deflections include independent lateral , vertical deflections (Fig. 2), which are parallel to the corresponding coordinate system of the track;
4) rail turning about axis is not considered;
5) the rail as a linear force element both in the lateral and vertical directions; the lateral dissipation is taken into account for two-point contact mode only.

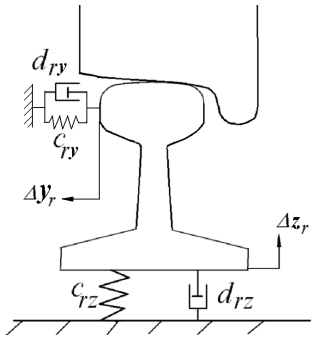

Fig. 2. Rail as massless force element [16]
Рис. 2. Рельс как безынерционный упруго-диссипативный силовой элемент [16]

Let c_{ry}, c_{rz} be the lateral and the vertical stiffness of the rail, d_{ry}, d_{rz} be the corresponding damping constants. Forces acting on the rail due to the deflections are the following:

$$R_y = -c_{ry}\Delta y_r - d_{ry}\Delta \dot{y}_r; \tag{1}$$

$$R_z = -c_{rz}\Delta z_r - d_{rz}\Delta \dot{z}_r. \tag{2}$$

Because the rail has no mass, these forces must be balanced by contact forces acting on the rail from the wheel. The contact forces acting on the wheel for one- and two-point contacts are shown in Fig. 3. Longitudinal forces are not shown in Fig. 3 (where: β_1, β_2 – the angles between the normal to the rail at contact and the axis perpendicular to the track).

Equilibrium equations for one-point contact written in coordinate system of the track are

$$\begin{aligned} R_y - F_1\cos\beta_1 + N_1\sin\beta_1 = 0, \\ R_z - N_1\cos\beta_1 + F_1\sin\beta_1 = 0. \end{aligned} \tag{3}$$

Analogous equations are valid for a two-point contact

$$\begin{aligned} R_y - F_1\cos\beta_1 + N_1\sin\beta_1 - F_2\cos\beta_2 + N_2\sin\beta_2 = 0, \\ R_y - N_1\cos\beta_1 + F_1\sin\beta_1 - N_2\cos\beta_2 + F_2\sin\beta_2 = 0. \end{aligned} \tag{4}$$

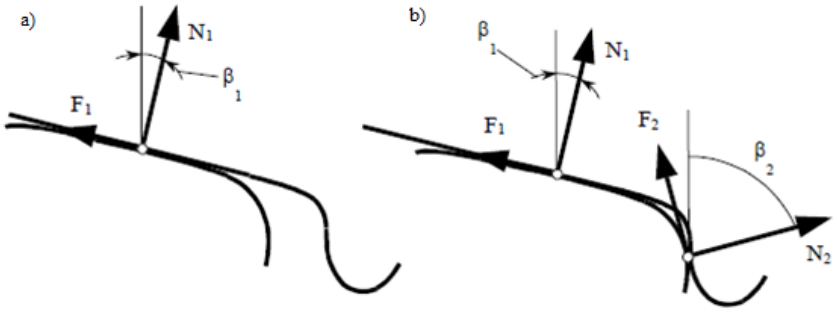

Fig. 3. Forces acting on wheel at one- and two-point contacts: a) one-point contact; b) two-point contact [16]
Рис. 3. Силы, действующие на колесо при одноточечном и двухточечном контакте [16]

Formula (3) for a one-point contact and formula (4) for a two-point contact are complicated systems of nonlinear algebraic equations relative to unknown deflections of the rail and normal reactions.

2.2. Algorithms for computing creep forces

The dynamic instability of railway vehicle bogies and wheel-sets is caused by the combined action of the conicity of the wheel running surface and the creep forces acting between the wheels and rails [15].

The effect of spin to the lateral creep force is approximated based on integration of the tangential stress caused by pure spin and on the results of Kalker's linear theory [4, 5]. The solution can be used for general conditions of longitudinal, lateral and spin creep. A detailed description of creep forces calculation and computer code can be found in [10].

Modern models of tangential forces in a wheel-rail contact are based on nonlinear dependencies of the general form:

$$F_x = F_x(N, \xi_x, \xi_y, \phi, p),\ F_y = F_y(N, \xi_x, \xi_y, \phi, p). \tag{5}$$

Here the following notations are used:
F_x, F_y – are the longitudinal and lateral creep forces lying in the tangential plane of the rail;
N – the normal force in the contact;
ξ_x, ξ_y – the longitudinal and lateral creepages;
ϕ – the spin of the wheel-set;
p – a set of geometrical parameters characterizing rail and wheel profiles, e.g. curvatures of contact surfaces in the case of the FASTSIM algorithm.

The normal contact force is calculated as [16]:

$$N = \frac{\delta \pi E}{2(1-\nu^2)} \cdot \frac{\int_{b_1}^{b_2} \left(\delta a - h(y) a - \frac{a^3}{6R} \right) dy}{\int_{b_1}^{b_2} \left[\left(\delta - h(y) + \frac{y^2}{4R} \right) \cdot \ln \left(\frac{a + \sqrt{a^2 + y^2}}{|y|} \right) - \frac{a}{4R} \sqrt{a^2 + y^2} \right] dy} \tag{6}$$

As it is known, the creepages and the spin satisfy the following relations:

$$\xi_x = v_x / v_0 \tag{7}$$

$$\xi_y = v_y / v_0 \tag{8}$$

$$\phi = \omega_n / v_0 \tag{9}$$

Where: v_x, v_y – are the corresponding components of sliding velocity at the contact point on the wheel relative to the rail; v_0 is the longitudinal velocity of the wheel-set; ω_n is the projection of the wheel angular velocity on the normal to the rail at the contact point. Models of the creep forces are used both for the one-point and for the two-point contact.

The FASTSIM algorithm is a general approach in that sense that its application area is not limited to the elliptical contact, but it can be used for an arbitrary area of contact; however in such case there is difficulty in computing compliance coefficients, since they are only well defined for elliptic area of contact.

Integration of tangents loads over the area of contact gives the resulting tangent loads [16]:

$$\begin{aligned} F_x &= \int_{y_r}^{y_l}\int_{-x_l}^{x_l} q_x(x,y)dxdy = -\frac{4R}{L_1}\xi_x\int_{y_r}^{y_l} g(y)dy + \frac{4R}{L_3}\psi\int_{y_r}^{y_l} yg(y)dy; \\ F_y &= \int_{y_1}^{y_2}\int_{-x_l}^{x_l} q_y(x,y)dxdy = -\frac{4R}{L_2}\xi_y\int_{y_r}^{y_l} g(y)dy + \frac{4\sqrt{2}}{3L_3}\psi\int_{y_r}^{y_l}[Rg(y)^{\frac{3}{2}}dy. \end{aligned} \tag{10}$$

FASTSIM solves a system of differential equations (in the adhesion area of the contact patch) or a system of differential-algebraic equations (in the sliding area of the contact patch) relative to tangential stresses. For this purpose the contact ellipse is divided into a number of narrow slices of the same width. In turn, each slice is divided into *n* elements of equal length within one slice (Fig. 4). Number of slices *m* and elements *n* is set by the user.

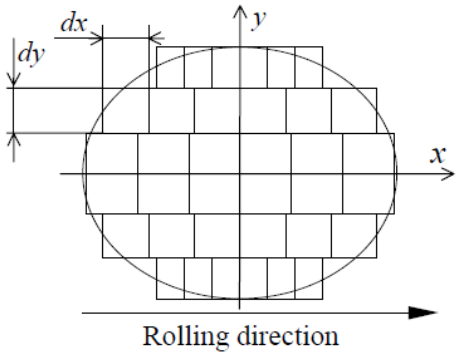

Fig. 4. Discretization of the contact ellipse
Рис. 4. Разбивка пятна контакта на полосы и элементы

FASTSIM solves the above mentioned equations for each of the slice successively to compute the creep forces and to obtain adhesion and sliding areas of the track.

3. MODELLING OF FREIGHT WAGON AND TRACK DYNAMICS

Freight wagons with three-piece bogies are widely used around the world in practice of heavy haul railway operations. The 18-100 model of the three-piece bogie is the standard bogie used in freight wagons of the Lithuania Railways. The following models of freight wagons with three-piece bogies were simulated with UM. The main difference of these models in contrast to similar models is

introducing friction wedges in the model as free bodies with six degrees of freedom (d.o.f.). Friction wedges interact with a side frame and a bolster by means of the point-plane contact model. A linear viscous-elastic model is used for the normal force in this contact model and stick-slip motion with two-dimensional friction in the tangent plane [16]. UM model of the three-piece bogie allows all clearances between the bolster, wedges, side frames and wheel-sets.

Investigated straight track 1000 m length of was modelled by UM software. Track irregularities were generated in accordance to PSD (spectral power density) function. The Rice-Pearson algorithm is used to generate the irregularity values by the equation:

$$x[n\Delta s] = \sum_{m=0}^{M} \sqrt{2S_c(m\Delta\omega)\Delta\omega}\cos\left[m\,\Delta\omega\; n\Delta s + \varphi(m\Delta\omega)\right]; \tag{11}$$

where: Δs is irregularity step size, m; M is the total number of harmonics in the sum;
$S_c(\omega)$ is the PSD function, m^2/(rad/m); $\Delta\omega$ is the frequency increment, rad/m; $\varphi(m\Delta\omega)$ is the phase uniformly distributed on interval $[-\pi, \pi]$.

Oscillograms of track irregularities are presented in Fig. 5 and Fig. 6.

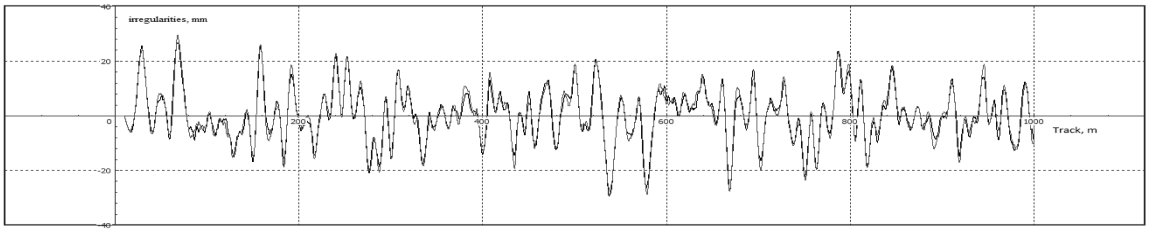

Fig. 5. Track irregularities on vertical flat
Рис. 5. Вертикальные неровности рельсовых нитей

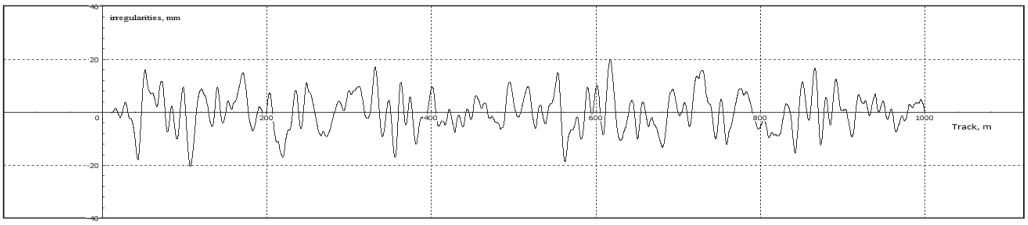

Fig. 6. Track irregularities on horizontal flat
Рис. 6. Горизонтальные неровности рельсовых нитей

Track stiffness and damping parameters were settled and the values are given in Table 1.

Table 1

Track stiffness and damping

	Straigth path	Curve
Vertical stiffness, MN/m	(10-90)	80
Lateral stiffness, MN/m	43	(5-90)
Vertical damping, kNs/m	440	440
Lateral damping, kNs/m	100	100

Generalised geometric parameters of the curves of Lithuanian Railways are given in Table 2.

Table 2

Geometric parameters of the curve

P_1, m	P_2, m	S, m	R, m	H, m
20	30	900	900	0.125

NOTE. P_1, P_2 – length of transient sections, S – length of steady curve section, R – radius of curve, H – super elevation of rail.

Two types of rail profiles were taken in this survey. Wheel and rail profiles are shown in Fig. 7.

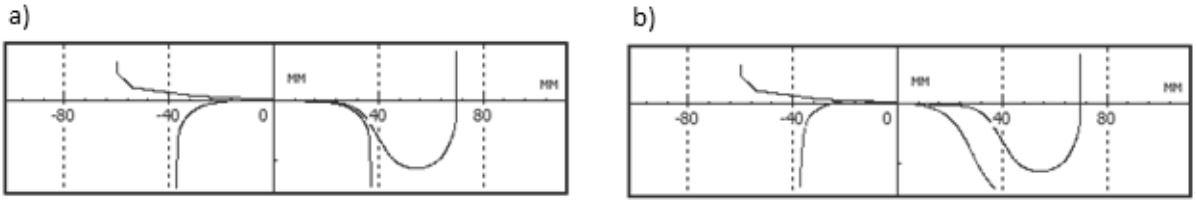

Fig. 7. Wheel and rail profiles: a) new wheel and new R65 rail; b) new wheel and old R65 with 13mm wear
Рис. 7. Профили колеса и рельса: а) новое колесо и новый Р65 рельс; б) новое колесо и Р65 рельс с 13 мм износом

Derailment occurs, when the wheel-set separates from the rail and cannot run anymore. It is one of the most dangerous occurrences affecting the safety of railway vehicles and must be prevented. Wheel-set derailment is one of the most dangerous occurrences affecting the safety of railway vehicles and must be prevented, especially for the high-speed vehicles [14]. The well-known Nadal's criterion treats wheel-climb derailments for normal driving using the lateral-to-vertical force limit ($L/V<0.85$) of a single wheel [13]. Nadal's wheel-climb derailments generally occur in situations where the climbing wheel experiences a high lateral force combined with a reduced vertical force.

Using UM package 609 imitation tests were carried out with the above-mentioned freight wagon running on the straight track and the comprehensive analysis of security criterion dependence on track stiffness changes was performed. Wagon was moving down the simulated track, which vertical and horizontal stiffness varied from 10 to 90 MN/m at different speeds and different axle load. Nadal's criterion changing was calculated for each wagon's wheel across of track stretch and the highest values were selected for the appropriate combination of track stiffness, wagon axle load and running speed values. After testing of the new rail profile R65 (Fig. 7a), it was changed to the old rail profile R65 with 13 mm attrition (Fig. 7b). Old (wear) rail profile R65 was tested only with straight track, not in curves. The creep forces were calculated by FastSim analytic method. The calculation results of Nadal's criterion are presented in Fig. 8 – Fig.17.

Fig. 8 and Fig. 9 shows that the running on new profile rails, Nadal's criterion reaches higher values than rolling on worn rails. The highest growth of criterion was observed, when 70 MN/m track stiffness is reached and axle load is q = 140 kN. When the axle load is higher, Nadal's criterion varies very slightly.

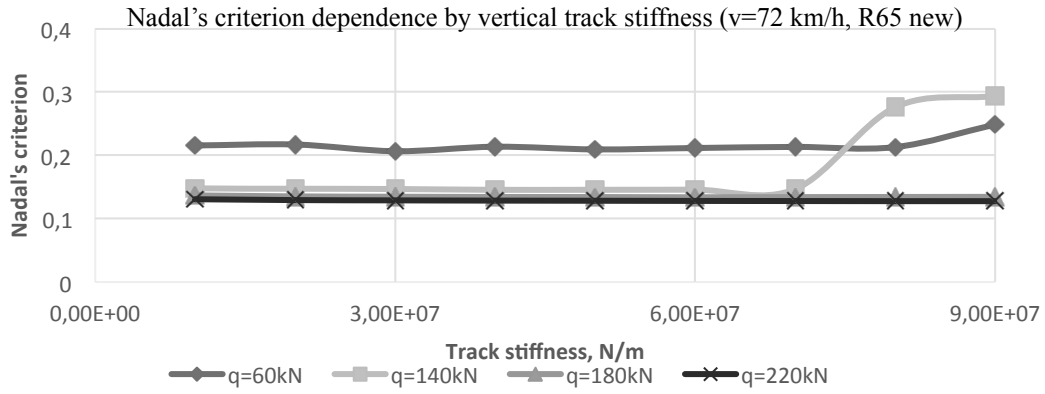

Fig. 8. Nadal's criterion dependence by vertical track stiffness (v=72 km/h, R65 new)
Рис. 8. Зависимость критерия Надаля от вертикальной жесткости железнодорожного пути (v=72 км/h, новый Р65)

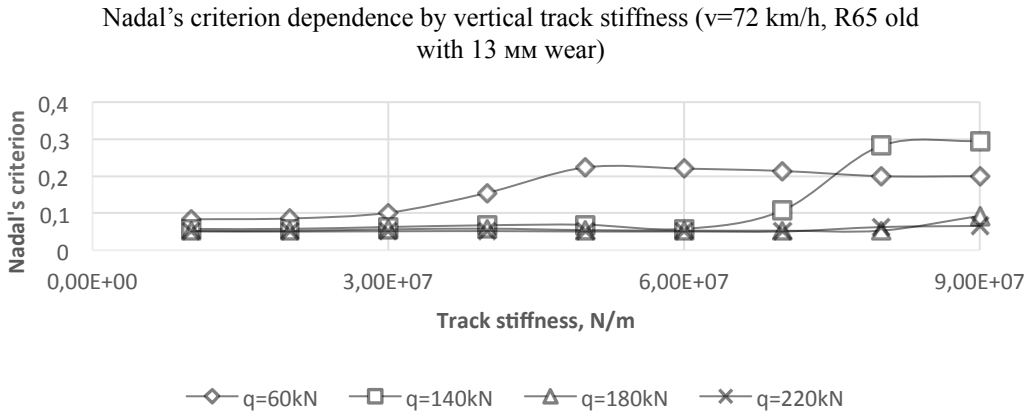

Fig. 9. Nadal's criterion dependence by vertical track stiffness (v=72 km/h, R65 old with 13mm wear)
Рис. 9. Зависимость критерия Надаля от вертикальной жёсткости железнодорожного пути (v=72 км/h, Р65 с износом 13 мм)

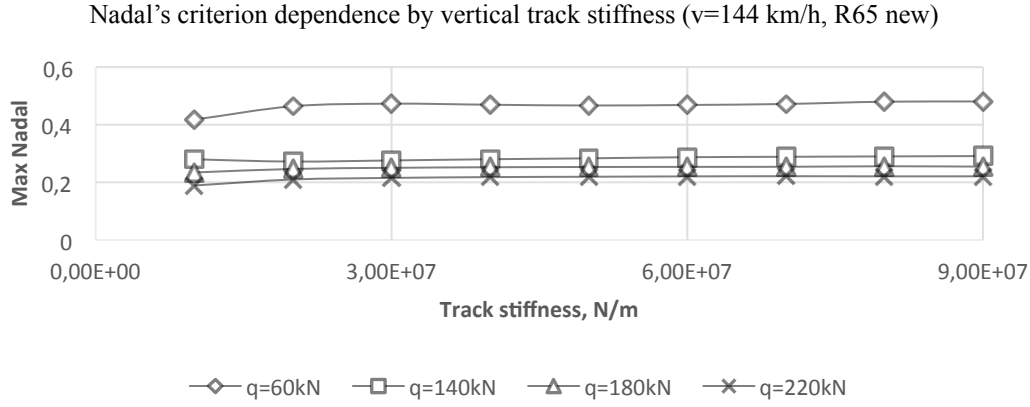

Fig. 10. Nadal's criterion dependence by vertical track stiffness (*v*=144 km/h, R65 new)
Рис. 10. Зависимость критерия Надаля от вертикальной жесткости железнодорожного пути (*v*=144 км/h, новый Р65)

Fig. 10 and Fig. 11 shows that the increase of speed up to 144 km/h, and running on a new profile rails, Nadal criterion depends more on the axle load changes than on the stiffness of the track, but when old rails are selected, a slight increase is observed when the criterion of track stiffness is 60-70 MN/m and axle load is larger than 140 kN. Maximum Nadal's criterion values obtained at 60 kN axle load on the 30 MN/m track stiffness.

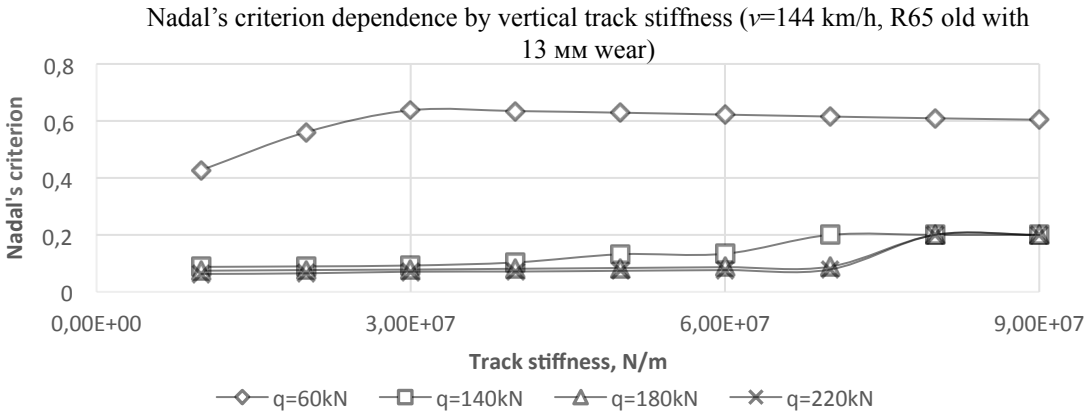

Fig. 11. Nadal's criterion dependence by vertical track stiffness (v=144 km/h, R65 old with 13 mm wear)
Рис. 11. Зависимость критерия Надаля от вертикальной жесткости железнодорожного пути (v=144 км/h, Р65 с износом 13 мм)

Fig. 12 and Fig. 13 shows that the Nadal's criterion exceeds the permissible limits for low-load axle. Dangerous criterion limits is reached when using a new rail profile and the stiffness of the track exceeds 30 MN/m. Safe movement on the old rails is not available.

When the load on axle exceeds 140 kN, the movement remains stable at any track stiffness values.

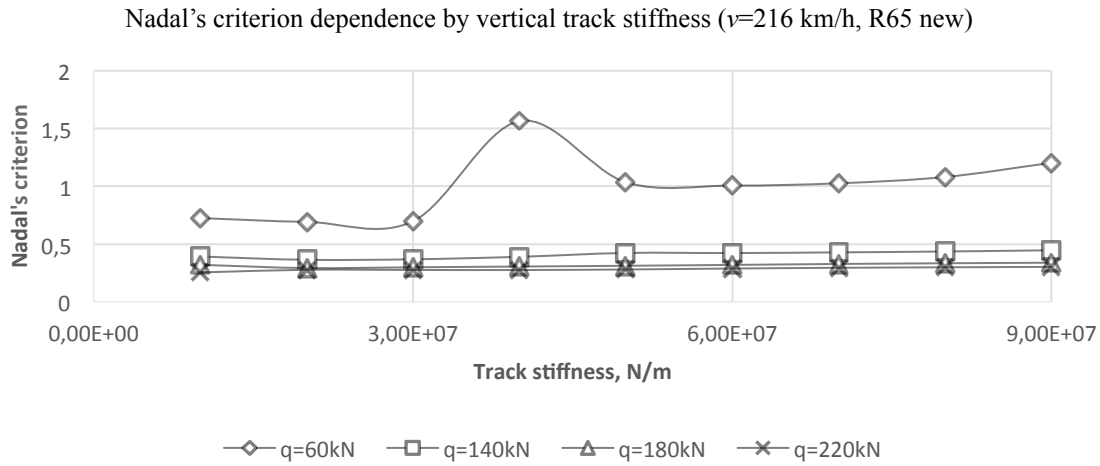

Fig. 12. Nadal's criterion dependence by vertical track stiffness (v=216 km/h, R65 new)
Рис. 12. Зависимость критерия Надаля от вертикальной жесткости железнодорожного пути (v=216 km/h, новый Р65)

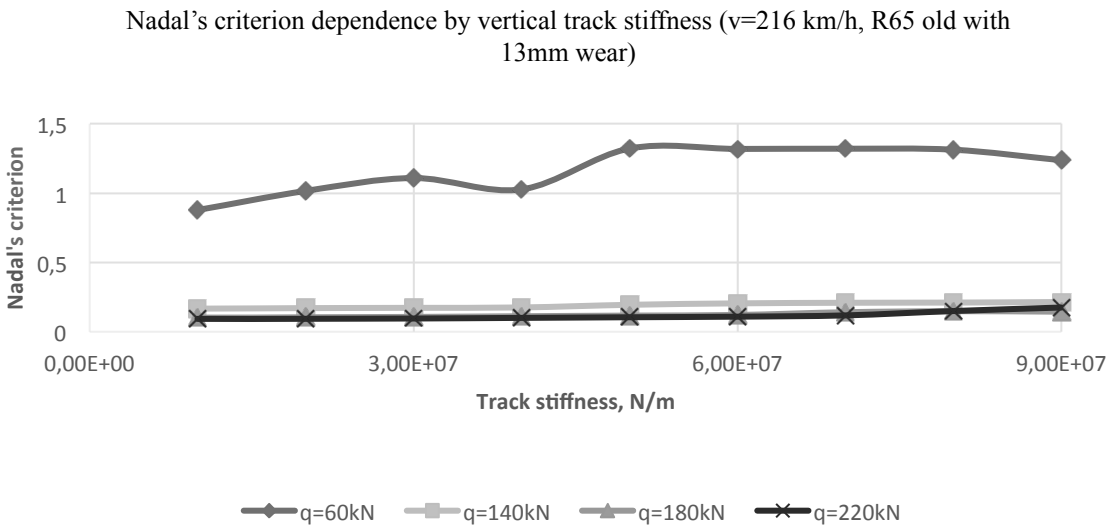

Fig. 13. Nadal's criterion dependence by vertical track stiffness (v=216 km/h, R65 old with 13 mm wear)
Рис. 13. Зависимость критерия Надаля от вертикальной жесткости железнодорожного пути (v=216 км/h, Р65 с износом 13 мм)

The examination of Fig. 14 and Fig. 15 shows that the safe movement is not available at q=60 kN load on axle on both types of rails profiles regardless of the track stiffness. Dangerous limit of Nadal's criterion is reached when running on the old rails at selected axle load 140 kN and the stiffness of the track exceeds 80 MN/m.

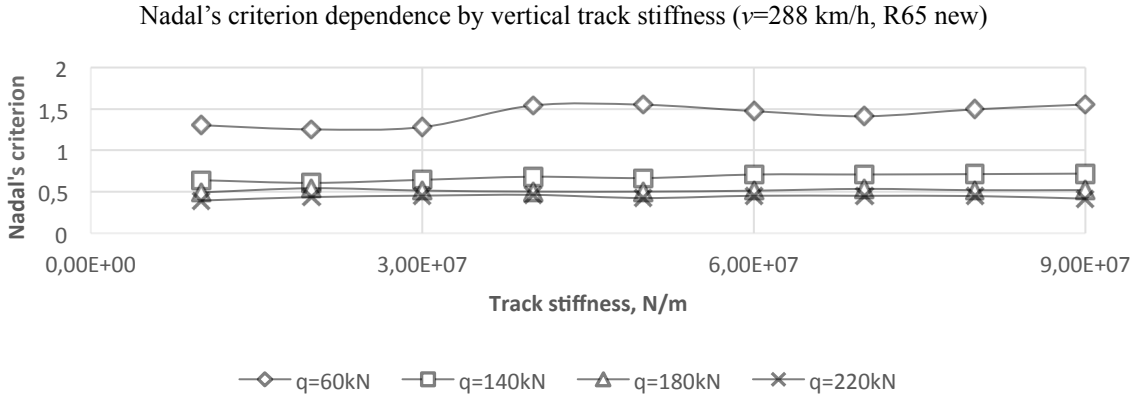

Fig. 14. Nadal's criterion dependence by vertical track stiffness (v=288 km/h, R65 new)
Рис. 14. Зависимость критерия Надаля от вертикальной жесткости железнодорожного пути (v=288 км/h, новый Р65)

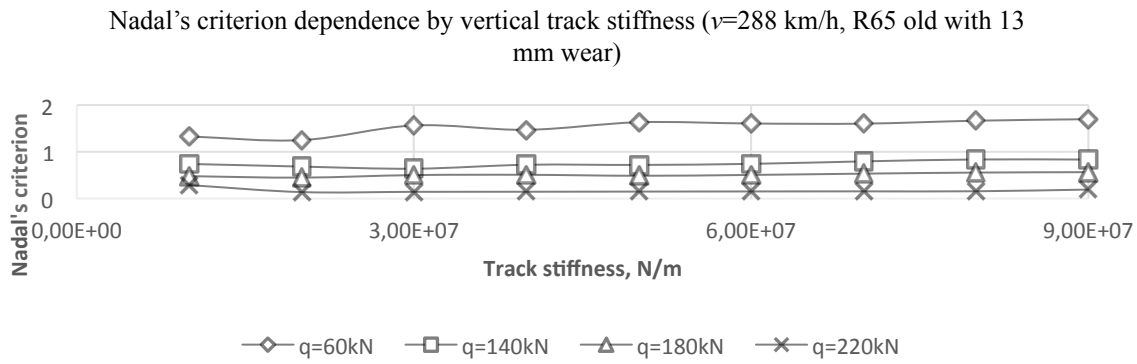

Fig. 15. Nadal's criterion dependence by vertical track stiffness (v=288 km/h, R65 old with 13 mm wear)
Рис. 15. Зависимость критерия Надаля от вертикальной жёсткости железнодорожного пути (v=288 км/h, Р65 с износом 13 мм)

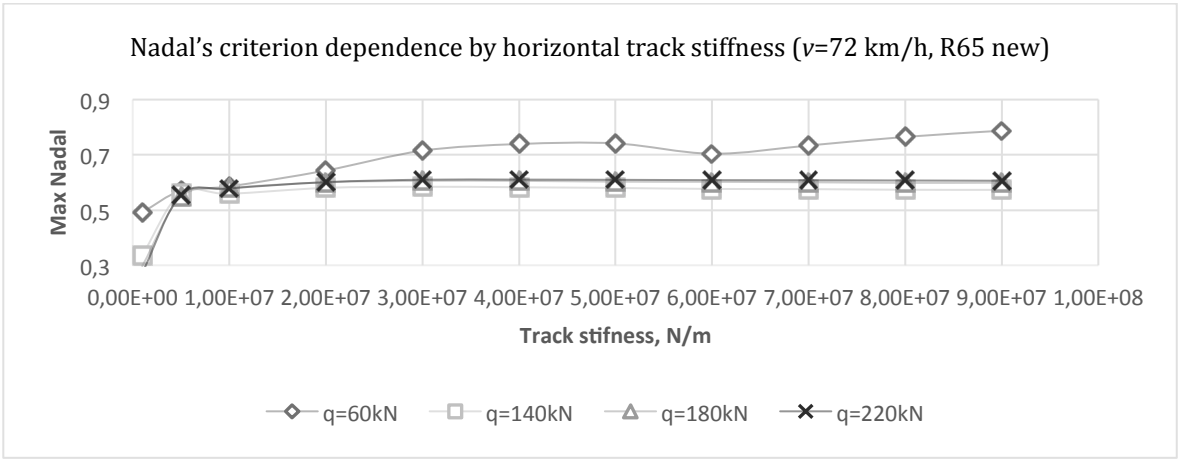

Fig. 16. Nadal's criterion dependence by track horizontal stiffness in curve (v=72 km/h, R65 new)
Рис. 16. Зависимость критерия Надаля от горизонтальной жесткости железнодорожного пути на кривой (*v*=72 км/h, новый Р65)

The diagrams in Fig. 16 shows that the safe movement of wagon is available at all horizontal stiffness of track, when axle load is more than 14 kN and horizontal stiffness is up to 80 MN/m. Additionally, Nadal's criterion approaches critical values, when wagon axle load is 6 kN.

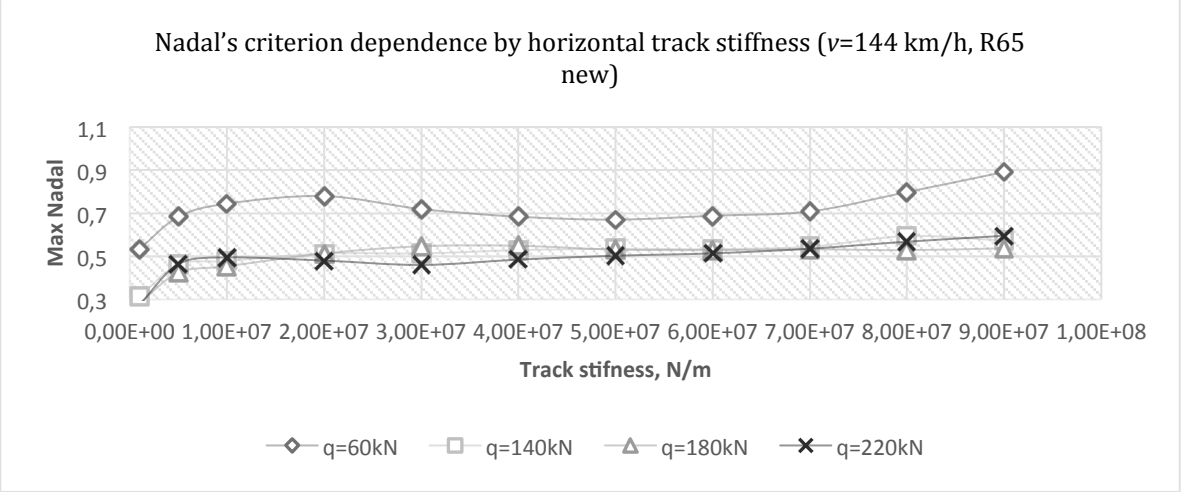

Fig. 17. Nadal's criterion dependence by horizontal track stiffness in curve (v=144 km/h, R65 new)
Рис. 17. Зависимость критерия Надаля от горизонтальной жесткости железнодорожного пути на кривой (v=144 км/h, новый Р65)

The diagrams in Fig. 17 show that the Nadal's criterion exceeds the permissible limits on track curves for low axle load (less than 60 kN), because of effect of quasi-static centrifugal forces. These forces reduce normal forces on inner rail and increase on outer rail. Furthermore, the quasi-static forces enhance the lateral (horizontal) pressure on outer rail as well.

Dangerous Nadal's criterion values are reached when using a new rail profile and the lateral stiffness of the track exceeds 80 MN/m. Nevertheless, as is shown in Fig. 17, the safest running of vehicle down the track curve is reached, when horizontal stiffness of track is (40-60) MN/m.

As further calculation showed, the derailment inevitably occurred, when the vehicle speed on track curve is more than 200 km/h.

4. CONCLUSIONS

1. By studying 4-axle freight wagon stability by software package UM it is possible to determine the ranges of safe running speed for empty and loaded wagons, taking into account track stiffness and its stage (new or wear rails).
2. During analysis of 4-axle freight wagon running modelling results it was found , that the Nadal's criterion of empty freight wagon is 1.5-2 times higher than the fully or partially loaded wagon. Moreover, when the speed is over 150 km/h, the Nadal's criterion of empty wagon running is almost critical or exceeds the critical value, especially at 216 km/h speed and more.
3. Partially loaded and fully loaded wagon's dynamic stability fluctuates much less when stiffness of track differs from 30 MN/m till 90 MN /m compare with empty wagon stability changes at all speed ranges.
4. The influence of track irregularities (rail wear of 13 mm) on partially or fully loaded wagon running stability was (2-3) times smaller compare with empty wagon stability.
5. After analysing of the results, it was observed, that the empty wagon running stability is almost consistent when the wagon runs at 144 km/h. Nevertheless, the Nadal's criteria value (0.5-0.65) in all cases was closed to critical 0.85.
6. Vertical track stiffness does not have perceptible influence on Nadal criterion value in curves.
7. The safest vehicle running down the track curve is reached, when horizontal stiffness of track is (40-60) MN/m.

8. Authors revealed some "protuberances" in Nadal's criterion diagrams (Fig.9 and Fig.10) of partially loaded wagon on the highest stiffness of track at 70 km/h speed and empty wagon on the average stiffness of track at 216 km/h speed (Fig.13). In the last case permissible value of Nadal's criterion exceeded 2 times. These unsearchable peaks on the Nadal's criterion diagrams are the goal for future investigation.

References

1. Ang, K.K. & Dai, J. Response analysis of high-speed rail system accounting for abrupt change of foundation stiffness. *Journal of Sound and Vibration.* 2013. Vol. 332(12). P. 2954-2970.
2. Baeza, L. & Vila, P. & Xie, G. & Iwnicki, S.D. Prediction of rail corrugation using a rotating flexible wheelset coupled with a flexible track model and a non-Hertzian/non-steady contact model. *Journal of Sound and Vibration.* 2011. Vol. 330. P. 4493-4507.
3. Fingberg, U.A Model of wheel-rail squealing noise. *Journal Sound Vibration*. 1990. Vol. 143. P. 365-377.
4. Kalker, J.J. A fast algorithm for the simplified theory of rolling contact. *Vehicle System Dynamics*. 1982. Vol. 11. P. 1-13.
5. Kalker, J.J. & Piotrowski, J. Some New Results in Rolling Contact. *Vehicle System Dynamics.* 1989. Vol. 18. P. 223-242.
6. Knothe, K. & Grassie, S.L. Modelling of railway track and vehicle track interaction at high frequencies. *Vehicle System Dynamics.* 1993. Vol. 22. P. 209-262.
7. Di Mascio, P. & Loprencipe, G. & Maggioni, F. Visco-elastic modeling for railway track structure layers. *Ingegneria Ferroviaria.* 2014. Vol. LXIX. No. 3. P. 207-222.
8. Metrikine, A.V. & Dietermann, H.A. The equivalent vertical stiffness of an elastic half-space interacting with a beam, including the shear stresses at the beam half-space interface. *European Journal of Mechanics A/Solids.* 1997. Vol. 16. P. 515-527.
9. Persson, R. & Andersson, E. & Stichel, S. & Orvnäs, A. Bogies towards higher speed on existing tracks. *International Journal of Rail Transportation.* 2014. Vol. 2(1). P. 40-49.
10. Polach, O. A fast wheel-rail forces calculation computer code. *Vehicle System Dynamics.* 1999. Vol. 33. P. 728-739.
11. Popp, K. & Kruse, H & Kaiser, I. Vehicle-track dynamics in the mid-frequency range. *International Journal of Vehicle Mechanics and Mobility.* 1999. Vol. 31. No. 5-6. P. 423-464.
12. Popp, K. Parametric excitation of a wheelset due to periodic normal forces. *Proc. 4th Polish-German Workshop.* Warsaw. 1996.
13. Seo, K.J. & Choi, S.Y. Theoretical development of a simplified wheelset model to evaluate collision-induced derailments of rolling stock. *Journal of Sound and Vibration.* 2012. Vol. 331(13). P. 3172-3198.
14. Steišūnas, S. & Bureika, G. & Liudvinavičius, L. Survey of assessment methods of rolling-stock chassis hunting and derailment processes. *The 8th International Conference TRANSBALTICA 2013.* 9-10 May 2013. Vilnius, Lithuania: Technika. 2013. P. 218-224.
15. Wickens, A.H. The dynamic stability of railway vehicle wheel-sets and bogies having profiled wheels. *International Journal of Solids and Structures.* 1965. Vol. 1(3). P. 319-341.
16. *Home page "Universal Mechanism"*. Available at: http://www.umlab.ru/en/pages/index.php?id=1.

Received 18.06.2013; accepted in revised form 04.12.2014